Published in final edited form as:
Pharm Res. 2014 November ; 31(11): 3106–3119. doi:10.1007/s11095-014-1403-6.

Evaluating the Anticancer Properties of Liposomal Copper in a Nude Mouse Xenograft Model of Human Prostate Cancer: Formulation, *In Vitro, In Vivo*, Histology and Tissue Distribution Studies

Yan Wang[1], **San Zeng**[1], **Tien-Min Lin**[1], **Lisa Krugner-Higby**[2], **Doug Lyman**[3], **Dana Steffen**[1], and **May P. Xiong**[1]

[1]School of Pharmacy, University of Wisconsin – Madison, Madison, Wisconsin 53705-2222, USA

[2]Research Animal Resources Center, University of Wisconsin-Madison, Madison, Wisconsin 53726, USA

[3]Wisconsin Veterinary Diagnostic Laboratory, Madison, Wisconsin 53706, USA

Abstract

Purpose—Although copper (Cu) complexes have been investigated as anticancer agents, there has been no description of Cu itself as a cancer killing agent. A stealth liposomal Cu formulation (LpCu) was studied *in vitro* and *in vivo*.

Methods—LpCu was evaluated in prostate cancer origin PC-3 cells by a metabolic cytotoxicity assay, by monitoring reactive oxygen species (ROS), and by flow cytometry. LpCu efficacy was evaluated *in vivo* using intratumoral and intravenous injections into mice bearing PC-3 xenograft tumors. Toxicology was assessed by performing hematological and blood biochemistry assays, and tissue histology and Cu distribution was investigated by elemental analysis.

Results—LpCu and free Cu salts displayed similar levels of cell metabolic toxicity and ROS. Flow cytometry indicated that the mechanisms of cell death were both apoptosis and necrosis. Animals injected i.t. with 3.5 mg/kg or i.v. with 3.5 and 7.0 mg/kg LpCu exhibited significant tumor growth inhibition. Kidney and eye were the main organs affected by Cu-mediated toxicities, but spleen and liver were the major organs of Cu deposition.

Conclusions—LpCu was effective at reducing tumor burden in the xenograft prostate cancer model. There was histological evidence of Cu toxicity in kidneys and eyes of animals treated at the maximum tolerated dose of LpCu 7.0 mg/kg.

Keywords

liposomes; copper; reactive oxygen species; cancer therapy; toxicity

INTRODUCTION

ROS are normal byproducts of metabolism and is usually kept under tight balance via intracellular redox reactions. ROS play a critical role in intracellular signaling and regulation of normal cellular processes (1). Most ROS are generated by the mitochondria during

metabolism of oxygen, but there is also evidence that NADPH oxidases contribute significant concentrations of ROS (2). Examples of ROS generated from oxygen are the superoxide anions ($O_2^{-}\cdot$), hydroxyl (·OH) free radicals, and hydrogen peroxide (H_2O_2), which is not a free radical but serves as an important source of ROS (3). Free radicals are atoms or molecules with unpaired electrons and are highly reactive. Excess ROS free radicals can cause intracellular damage by interacting with lipids and nuclear DNA, and can lead to denaturation or direct cleavage of proteins (3).

Of particular interest to us is the interaction between the un-reactive H_2O_2, which can cross biological membranes, with intracellular transition metals (such as Cu or iron) in what is known as the Fenton reaction (4); this reaction leads to the generation of highly reactive and cell damaging hydroxyl free radicals inside cells (5). ROS are present in various types of cancers at higher concentrations than in normal cells and such free radicals can play dual roles in cancer cell survival by stimulating cell proliferation and promoting tumorigenesis, destabilizing genes, and inducing adaptive responses (6); however, when the intracellular redox homeostasis of cancer cells is disturbed above a critical threshold, elevated concentrations of ROS can lead to significant disruptions in cellular processes and result in cell death (6).

Cu is a potential therapeutic transition metal for the generation of cytotoxic concentrations of ROS in cancer cells, and may potentially exhibit low side effects in normal tissues due to presence of various homeostatic mechanisms for import/export of Cu from the body. More specifically, several proteins have been identified that may play very important roles in Cu import and export in mammalian cells: copper transport protein CTR1 is a high affinity transporter protein found in the plasma membrane and in lysosomes/endosomes that is thought to be critical for the regulation and import of Cu into cells (7). Copper transport protein CTR2 is thought to be a low affinity transporter for the import of Cu and is predominantly also found in lysosomes/endosomes (7). Examples of Cu efflux transporters are the copper-transporting ATPase ATP7A which releases Cu into the bloodstream and copper-transporting ATPase ATP7B which releases Cu into the bile for excretion by the body. Both ATPases transport Cu into intracellular vesicles that fuse with the plasma membrane for indirect Cu release (7).

Drug delivery systems (DDS) such as liposomes can be utilized to formulate Cu. Formulation of a drug into a DDS can improve pharmacokinetic and pharmacological effects of the drug (8). Liposomes possess several advantages for encapsulation of the salt form of Cu. They can be easily fabricated to various sizes depending on desired *in vivo* behavior, are preferable for encapsulation of hydrophilic or amphiphilic small molecules, and can be easily modified for PEGylation or incorporation of a targeting ligand (9). The size of a liposome plays a very important role in prolonging circulation *in vivo*. It has been reported that liposomes averaging 100 nm in diameter have remarkably longer circulation times in rat blood compared to larger-sized liposomes (10). This prolonged circulation has been suggested to be due to small liposomes passing through fenestrations present in the hepatic sinusoidal endothelium of the liver (11), enabling them to evade phagocytosis by Kupffer cells. In the absence of targeting ligands, most DDS of appropriate size can preferentially target malignant tissues over normal organs by taking advantage of the

Enhanced Permeability and Retention (EPR) effect (12). The EPR effect depends on the defective and leaky blood vasculature and poor lymphatic drainage of tumor tissues for extravasation of nanoparticles into the tumor area, typically absent in normal vasculature. Although Cu complexes have been synthesized as anticancer agents (13, 14), the potential therapeutic effect of Cu itself has not yet been investigated. The mechanism of action for different Cu complexes varies. A Cu complex bearing a 3-formylchromone thiosemicarbozone ligand inhibited PKB (an Akt protein) activity and caused NF-κB inactivation in K-ras mutant human pancreatic COLO-357 cancer cells, leading to significant tumor reduction in an established orthotopic animal model of pancreatic cancer (15). Another study reported on two isatin-Shiff base Cu complexes with pro-apoptotic activity. Interestingly, the extent of apoptosis induced in SH-SY5Y neuroblastoma cells correlated with intracellular Cu uptake (16). Although highly potent, these novel Cu complexes suffered from poor water solubility and bioavailability, which could significantly limit their pharmaceutical development.

Here, a stealth liposomal formulation of Cu (LpCu) was prepared and its anticancer properties in relation to metabolic toxicity, ROS production, and cell death mechanism were characterized in cultured PC-3 prostate cancer cells. The antitumor efficacy of the formulation was evaluated in a PC-3 xenograft tumor mouse model. Tissue distribution of Cu, histology, and hematologic analyses in animals are also reported.

MATERIALS AND METHODS

Materials

Copper chloride ($CuCl_2$), copper sulfate pentahydrate ($CuSO4{\cdot}5H_2O$), bicinchoninic acid disodium salt hydrate (BCA), resazurin sodium salt and *tert*-butyl hydroperoxide (TBHP) were purchased from Sigma-Aldrich (St. Louis, MO). Dipalmitoylphosphatidylcholine (DPPC), dipalmitoylphosphoethanolamine-N- [methoxy(polyethylene glycol)-2000] ammonium salt (DPPE-PEG_{2000}) and cholesterol were purchased from Avanti Polar Lipids (Alabaster, AL). Dulbecco's Modified Eagle Medium (DMEM), Dulbecco's phosphate buffered saline (DPBS), Hank's balanced salt solution (HBSS), fetal bovine serum (FBS) and 1% penicillin/streptomycin were purchased from Cellgro (Manassas, VA). The fluorescent dye 2',7'-dichlorodihydrofluorescein diacetate (H_2DCFDA) was purchased from Life Technologies (Grand Island, NY). DC protein assay kit was purchased from BIO-RAD (Hercules, CA). For flow cytometry, Annexin V-FITC apoptosis detection kit I containing propidium iodide was purchased from BD Biosciences (San Jose, CA). Alanine aminotransferase (ALT), aspartate aminotransferase (AST) and creatinine (Cr) ELISA kits were purchased from MyBioSource (San Diego, CA). All other chemicals were reagent grade or better.

Preparation of Stealth Liposomal Cu (LpCu)

Stealth liposomes were prepared by the hydration-extrusion method by incorporating 5% PEGylated lipids (DPPE-PEG_{2000}) into the total phospholipid concentration (17). Briefly, lipid mixtures of DPPC, cholesterol and DPPE-PEG_{2000} at a molar ratio of 80:50:4 (μmol) were dissolved in chloroform and the solvent was evaporated on a rotary evaporator under

vacuum. Non-PEGylated liposomes were prepared without the addition of DPPE-PEG_{2000}. Next, 100 mM (or other concentrations) of $CuCl_2$ (or $CuSO_4$) solution was used to hydrate the thin film of lipids that formed on the wall of the round bottom flask, while rotating in a 55 °C water bath for 30 minutes. The resulting multilamellar vesicle (MLV) suspension was subjected to three freeze-thaw cycles before being extruded 11 times through a 100 nm polycarbonate membrane filter (Whatman, Springfield Mill, UK) via a Mini-Extruder Set (Avanti Polar Lipids) to generate large unilamellar vesicles (LUVs) encapsulating the Cu salt. Residual un-encapsulated Cu was removed by size exclusion chromatography by passing the suspension through a desalting PD-10 column (GE Healthcare, Waukesha, WI) and eluting with either ddH_2O (for short-term storage and *in vitro* experiments) or 0.9% sodium chloride (for *in vivo* administrations into mice). Saline liposomes were prepared by encapsulating normal saline solution instead of $CuCl_2$ solution.

Encapsulation Efficiency of Cu in Liposomes

A modified colorimetric assay was used to determine Cu concentration in the liposomal suspension (18). Briefly, an aliquot of sample (1–5 μl) was dissolved in 20 μl methanol and diluted with ddH_2O (~1 ml) to release encapsulated Cu from liposomes. Next, Cu^{2+} was reduced to Cu^{+} with ascorbic acid and 1 ml of 0.2 mM BCA was added to the solution (forming a stable purple complex with Cu^{+}). The absorption of the samples were measured at 562 nm with a SpectraMax Plus absorbance microplate reader (Molecular Devices, Sunnyvale, CA) and readings were fit to a standard linear calibration curve to calculate the concentration of Cu encapsulated in liposomes. Encapsulation efficiency (EE) was calculated by the following equation:

For example, when 1 ml 100 mM $CuCl_2$ was used to rehydrate lipids, 2 ml LpCu suspension was obtained after eluting the suspension through the PD-10 column, for a Dilution Factor (DF) of 2. For 100 mM $CuCl_2$, the final Cu encapsulation level was found to be 9.65±0.35 mM, as measured by the colorimetric assay (Table 1), and therefore the EE calculated was 19.3±0.7%.

Characterization of LpCu

A Zetasizer Nano ZS (Malvern Instruments, UK) was used for dynamic light scattering (DLS) and zeta-potential measurements. The cumulant diameters of samples were calculated by the Stokes-Einstein equation (automatically calculated by instrument software) and are reported as Z-average diameters. The instrument also generated a polydispersity index (PDI) for each sample, indicative of the particle size distribution. Zeta-potentials were measured with U-shaped disposable capillary cells. Three separate measurements were conducted for each formulation and results reported as mean ± standard deviation (MEAN±SD). Colloidal stability of LpCu in pure serum was assessed by incubating 0.1 ml LpCu formulations in 3 ml FBS at 37 °C for up to 48 hours and monitoring particle size distribution of samples with DLS at 0, 24 and 48 hour time points.

In Vitro Release Studies

A 1 mL aliquot of various LpCu suspensions were sealed in dialysis membranes (MWCO 10,000) and dialyzed against 1000 mL of 0.9% NaCl solution at 4 °C, 25 °C and 37 °C. The

outer solution was refreshed every 12 hours to mimic sink conditions. A 10 μl aliquot of LpCu from each formulation was removed from the dialysis bag at the indicated time points, to assay for Cu concentration (via the colorimetric assay). Results reported are the average of triplicate experiments.

Cell Metabolic Viability Studies

The PC-3 human prostate cancer cell line was obtained from American Type Culture Collection (ATCC, Rockville, MD). Cells were cultured at 37 °C/5% CO_2 in DMEM supplemented with 10% (v/v) heat-inactivated FBS, 2 mM L-glutamine, 100 U.I./ml penicillin and 100 μg/ml streptomycin. Cells were seeded into 96-well plates at a density of 5000 cells per well and allowed to adhere for 24 hours prior to the cytotoxicity assay. Cell viability was measured by a resazurin-based metabolic assay (19). Specifically, after 24 hours of exposure to Cu or LpCu, 10 μl resazurin PBS solution (440 μM) mixed with 90 μl of antibiotic-free DMEM containing 10% FBS were added to each well and incubated for 2 hours. The fluorescence in each well was read with a SpectraMax Gemini EM microplate reader (Molecular Devices, Downingtown, PA) by excitation at 560 nm and emission at 590 nm. Readings from wells without cells were used as blanks. The reading taken from control cells (only medium added) or $E_{control}$ represented 100% cell viability and sample viability was calculated as $E_{sample}/E_{control}\times 100\%$. Since resazurin is non-toxic to cells, the medium was substituted with fresh antibiotic-free, serum containing-DMEM and incubated at 37 °C for another 24 hours prior to measuring cell viability at the 48 hour time point (measured again via the resazurin assay).

Intracellular ROS Production

Intracellular concentrations of ROS were quantified with the pro-fluorescent substrate H_2DCFDA (20). Briefly, PC-3 cells were seeded into 96-well plates at a density of 25,000 cells per well and allowed to adhere for 24 hours. Afterwards, cells were incubated with 100 μl of 25 μM H_2DCFDA in DPBS buffer for 30 minutes. The cells were washed with DPBS to remove extracellular H_2DCFDA prior to addition of the formulations (suspended in 10% FBS/DMEM). The oxidizing agent TBHP was added to wells at a final concentration of 100 μM and was used as the positive control. LpCu and $CuCl_2$ were added to wells at a final concentration of 122 and 154 μM respectively; concentrations chosen corresponded to respective IC_{50} as determined by the metabolic cell viability studies. Intracellular cleavage and oxidization of the pro-fluorescent substrate H_2DCFDA into its active fluorescent form 2',7'-dichlorofluorescein (DCF) correlates directly with intracellular levels of ROS. The fluorescence intensity was measured (Ex/Em = 485/535 nm) at 1.5, 6, 24 and 48 hour time points following addition of Cu or LpCu. At each time point, total protein concentration was also measured for each well using the BIO-RAD DC protein assay kit; resulting fluorescence readings normalized to total protein concentrations are reported for the different treatment groups.

Cell Death Mechanism Study with Flow Cytometry

PC-3 cells were seeded in 60 cm^2 cell culture dishes and incubated at 37 °C/5% CO_2 for 24 hours. Cells were then treated with either 122 μM LpCu or 154 μM $CuCl_2$ (at their IC_{50}), or PBS as the negative control. After 48 and 72 hours of incubation with the formulations, both

dead and live cells were collected, washed with PBS, and resuspended in binding buffer (10 mM HEPES/NaOH, pH 7.4, 140 mM NaCl, 2.5 mM $CaCl_2$) at a final concentration of 1×10^6 cell/ml. Next, 1×10^5 cells were stained with the Annexin V-FITC apoptosis detection kit I by incubating at room temperature for 15 minutes. Then, 400 μl binding buffer was added to each sample and the cells were analyzed with a FACSCalibur flow cytometer. The data was analyzed with FlowJo® software (version 10.0.6).

Antitumor Efficacy

PC-3 cells were allowed to reach 70% confluence on 60 cm^2 plastic tissue culture plates before harvesting. Approximately 1×10^6 cells suspended in 100 μl HBSS were inoculated subcutaneously into the right flanks of 8-week-old male athymic nude mice (Harlan Laboratories, Indianapolis, IN). When tumors reached a size of about 50 mm^3, animals were randomly divided into two groups (n=6) and administered either a solution of LpCu at 3.5 mg/kg or normal saline by i.t. injections; mice were treated every four days for a total of three doses. In another set of animal experiments, PC-3 tumor-bearing nude mice were randomized into five groups (n=5 or 6) and administered LpCu at 3.5 mg/kg, LpCu at 7 mg/kg, $CuCl_2$ at 3.5 mg/kg, saline in liposomes, or saline by i.v. injections every four days for a total of three doses. Animals that displayed signs of severe acute toxicities (weight loss, hunched posture, and/or reluctance to move) were promptly euthanized prior to collection of blood and tissue samples. All tumors were measured daily with a caliper and tumor volume was calculated as an ellipse by using the following formula: volume = $\pi \times abc/6$, where a, b and c are the orthogonal diameters of tumor. Animal body weights were also monitored daily to assess for evidence of acute toxicities. All animal experiments were performed in accordance with the guidelines and protocols approved by the University of Wisconsin-Madison's Institutional Animal Care and Use Committee.

Blood Analysis, Histology, Tissue Cu Concentration and Distribution

At the end of the antitumor efficacy study, animals injected i.v. with LpCu formulations were euthanized by carbon dioxide inhalation, and blood and serum samples were collected. Complete blood counts were obtained with a VetScan HM2 system. ALT, AST and Cr serum concentrations for all animals were initially analyzed with respective ELISA kits by following manufacturer protocols, but unfortunately ELISA kits did not give results in standard units so samples within the same treatment groups were pooled and sent in for analysis by the Clinical Pathology Laboratory of the Veterinary Medical Teaching Hospital at the University of Wisconsin-Madison.

Several different organs were collected for histology and tissue analysis. For histology: lung, brain, liver, spleen, kidney, eye and tumor tissues were fixed in 10% buffered formalin solution, processed for histology by sectioning at 5 μm, and stained with hematoxylin and eosin. Microscopic images were acquired on an Olympus BX-51 microscope. Tissue slides were analyzed by a diagnostic pathologist at WVDL.

For Cu concentration and distribution studies, liver, spleen, kidney, eye and tumor tissues from animals within the same treatment groups were pooled and sent to WVDL for

elemental analysis by ICP/MS to quantify Cu levels in the different organs. Results reported are based on wet weight of the tissue.

Statistical Analyses in Animal Studies

In the antitumor efficacy studies, data are presented as mean ± standard error of the mean (MEAN±SEM). A two-way ANOVA was used to compare tumor growth rates by evaluating the statistical difference between treatment and control groups; a $p < 0.05$ was considered statistically significant. Prism 5 software (GraphPad, San Diego, California) was used for all analyses and graphs.

RESULTS

Preparation of LpCu

Formulations of LpCu, two Cu salts $CuCl_2$ and $CuSO_4$ at concentrations ranging from 100 to 500 mM were investigated (Table 1). The EE for both Cu salts was very similar, with values ranging from 19–21% regardless of the salt form or initial Cu concentration. All the formulations were prepared by the hydration-extrusion method and had similar narrow size distributions with PDI < 0.1. The formulations were characterized by mean diameters of about 148 nm with PDI of 0.075 for $CuCl_2$ and 146 nm with PDI of 0.069 for CuSO4. Similarly, the zeta-potential of all the formulations ranged from −6 to −10 mV after PEGylation and was slightly negative due to presence of the DPPE-PEG_{2000} on the liposomal surface (DPPE contains an anionic head group). Due to the high aqueous solubility of Cu salts, Cu ions distributed evenly both within and outside of liposomes regardless of the initial Cu concentration. As a result, the EE of Cu was mainly determined by the internal aqueous capture volume of liposomes, which is dependent on lipid composition, size, morphology and lamellarity (21). For example, for 134 μmol of total lipids utilized in each liposomal preparation and an average EE of 20%, approximately 0.2 of every 1.0 ml aqueous volume was entrapped by liposomes; dividing the encapsulated volume by the mole quantity of lipids resulted in a unit capture volume of 1.5 μl/μmol for the formulations. This unit capture volume estimate is in agreement with other reported values for LUVs (21).

Physical Characterizations

The colloidal stability of LpCu in pure serum was assessed by incubating liposomes in FBS at 37 °C and monitoring for signs of aggregation by DLS for up to 48 hours (Table 2). Immediately after incubation, the mean diameter of liposomes encapsulating $CuCl_2$ averaged 163 nm with PDI of 0.171 and 168 nm with PDI of 0.159 for $CuSO_4$; the larger PDI indicated wider size distributions. The diameters were also slightly larger than those dispersed in aqueous media (Table 1) and the differences were most likely due to the adsorption of serum proteins onto the liposomal surface in spite of the presence of PEG. The mean diameter for liposomes encapsulating $CuCl_2$ and $CuSO_4$ after 24 hours of incubation was 160 nm with PDI of 0.175 and 166 nm with PDI of 0.163 respectively. The mean diameter for liposomes encapsulating $CuCl_2$ and $CuSO_4$ after 48 hours was 162 nm with PDI of 0.180 and 167 nm with PDI of 0.169 respectively. There was no aggregation or

dramatic changes in the size distributions for the formulations when incubated in pure serum at 37 °C.

In vitro release properties of LpCu were evaluated at 4 °C, 25 °C and 37 °C. The *in vitro* release study was conducted using various concentration of Cu in liposomes; final Cu concentrations encapsulated ranged from about 10–50 mM for both $CuCl_2$ and $CuSO_4$ (based on EE of 100–500 mM initial Cu solutions, Table 1). The release profiles of Cu from LpCu, for both Cu salt forms, were independent of the encapsulated Cu concentration. When dialyzed at 4 °C, ca. 4% Cu was released after 72 hours and < 7% released after two weeks (only release data for the first 3 days is shown in Fig. 1); when LpCu samples were stored in glass vials at 4 °C instead of being dialyzed against 0.9% NaCl solution, Cu release was < 1% after two weeks (data not shown). At 25 °C, the release of Cu from LpCu was < 20% after 72 hours of dialysis against 0.9% NaCl. The release of Cu from liposomes at 37 °C proceeded at a much faster rate, with an approximate time to 50% release ($t_{1/2}$) of about 30 hours and 95% release after 72 hours. The release profiles and half-lives were nearly identical for all the formulations at all concentrations tested (see Supplemental Information, Fig. 1s). A representative set of release profile for LpCu prepared from 100 mM $CuCl_2$ is shown (encapsulated Cu concentration ~10 mM) (Fig. 1).

Cytotoxicity of LpCu

The *in vitro* metabolic cytotoxicity of LpCu formulations was assessed on PC-3 cells after 24 and 48 hour incubations (Fig. 2). Cytotoxicity data were very similar for both Cu salt forms. The IC_{50} of $CuSO_4$ after 24 and 48 hours decreased from 327 to 136 μM and the IC_{50} of $CuSO_4$ formulated in liposomes decreased from 585 to 167 μM (Fig. 2a, 2b). Similarly, the IC_{50} of $CuCl_2$ decreased from 302 to 154 μM and the IC_{50} of $CuCl_2$ formulated in liposomes decreased from 383 to 122 μM respectively (Fig. 2c, 2d). *In vitro*, there was no significant difference in cytotoxicity between the free salt form of Cu and LpCu. Due to the similar cytotoxicity results, only LpCu formulated with the $CuCl_2$ salt was investigated further. The effect of PEGylation (Fig. 2s), incubation time (Fig. 3s) and serum concentration (Fig. 4s) on the cytotoxicity of LpCu and free Cu were also investigated (see Supplemental Information). Results indicated that incorporation of PEG did not inhibit uptake of stealth liposomes compared to un-PEGylated liposomes, both formulations had similar antiproliferative effects. The length of incubation time with LpCu and $CuCl_2$ was more critical. The 24-hour incubation time resulted in greater metabolic cytotoxicity than 4-hour incubation time. Decreasing the serum concentration in media from 10% to 2% did not affect LpCu cytotoxicity, but free Cu cytotoxicity was increased in reduced serum.

Intracellular ROS

An assay to detect the presence of free radicals in cells treated with $CuCl_2$ and LpCu was used to investigate whether the uptake of Cu by cells could increase intracellular ROS concentrations. The pro-fluorescent substrate H_2DCFDA is deacetylated to H_2DCF after entering cells, and only becomes oxidized to the more fluorescent DCF form in the presence of intracellular ROS; keeping in mind that oxidation of H_2DCFDA is not specific to any particular free radicals, the assay can be utilized to quantify overall concentrations of ROS generated in cells over time. Untreated PC-3 cells were used as negative controls. Cells

treated with the oxidizing agent TBHP at 100 μM final concentration was the positive control, and LpCu and $CuCl_2$ were added to cells at their respective IC_{50} concentrations (122 and 154 μM respectively). Addition of TBHP to cells resulted in immediate ROS production within 1.5 hours of treatment, with a gradual increase over 48 hours (Fig. 3). Similarly, LpCu and $CuCl_2$ treatments induced a slower, gradual increase of cellular ROS up to 48 hours. There was significantly more ROS at 24 hours generated in cells treated with LpCu compared to $CuCl_2$ ($p < 0.01$), but this difference did not reach statistical significance at 48 hours ($p > 0.05$). Compared to the negative control group, LpCu treatment resulted in 3.5 and 3.9 fold production of ROS at 24 and 48 hour time points ($p < 0.01$), respectively. $CuCl_2$ treatment resulted in 2.9 and 3.8 fold production of ROS at the 24 and 48 ($p < 0.01$) hour time points respectively compared to the negative control.

Mechanism of Cell Death

Flow cytometry was utilized to probe for evidence of cell cycle arrest but there was no evidence of this mechanism noted in control or treatment groups (see Supplemental Info, Fig. 5s). A flow cytometry assay was used to probe for both apoptosis and necrosis after incubating cells with LpCu or $CuCl_2$ for 48 and 72 hours. Both live and dead cells were collected and stained with Annexin V-FITC and PI. In apoptotic cells, the membrane phospholipid phosphatidylserine (PS) is translocated from the inner to the outer leaflet of the plasma membrane, allowing for Annexin V protein to specifically bind exposed PS; viable cells with intact membranes exclude PI whereas the membranes of dead and damaged cells are permeable to PI. Therefore, viable cells become both Annexin V-FITC and PI negative; cells in the early apoptosis stage become Annexin V-FITC positive and PI negative; cells that are in late apoptosis or already dead become Annexin V-FITC and PI positive; necrotic cells become Annexin V-FITC negative and PI positive. More than 90% control PC-3 cells (untreated) were viable both at 48 and 72 hours whereas all cells treated with $CuCl_2$ and LpCu displayed evidence of apoptosis; a population of cells treated with LpCu (but not $CuCl_2$) was also found to be necrotic, indicating that LpCu induced both apoptosis and necrosis in PC-3 cells (Fig. 4).

Antitumor Efficacy of LpCu

The *in vivo* antitumor efficacy of LpCu was investigated via both the i.t. and i.v. routes in a PC-3 xenograft nude mouse tumor model. Approximately 3.5 mg/kg of LpCu was directly injected into the tumor (i.t.) after tumors reached an initial size of 50 mm^3. A total of three treatments were given on Days 0, 4, and 8 (Fig. 5a). Compared to saline treated mice, tumor volumes were significantly reduced by Day 12. The mean tumor volume of treated mice was ca. 44% smaller than that of control groups after the three injections ($p < 0.01$). No acute toxicity was observed for LpCu at the concentration administered (Fig. 5b); a body weight loss of 15% would have indicated acute toxicity in animals.

Prior to investigating the antitumor efficacy of LpCu by i.v. administration, a maximum tolerated dose (MTD) study was conducted by injecting escalating doses of LpCu encapsulating 10–50 mM Cu (formulated from initial Cu stock of 100–500 mM) and corresponding to 3.5–17.5 mg/kg (same injection volume) into normal mice; the MTD was found to be 7.0 mg/kg and was defined as the highest dose of LpCu that could be safely

administered to animals without causing death or obvious side effects. When higher dosages of LpCu were injected (formulated from initial 300, 400, or 500 mM $CuCl_2$), severe toxicities were observed after a few days and resulted in the death or euthanasia of the mice. Subsequently, two LpCu dosages, 3.5 mg/kg and 7.0 mg/kg, were tested in tumor bearing mice. A total of three treatments on Days 0, 4 and 8 were administered by i.v. injection after the tumor reached a size of 50 mm^3. Free $CuCl_2$ were also administered to tumor bearing mice at a dose of 3.5 mg/kg, however, two out of five mice were found dead three days after the first dose, and the other three were hunched and lethargic, so $CuCl_2$ administrations was discontinued and the mice in this group were euthanized at day 4. Both LpCu 3.5 mg/kg and 7.0 mg/kg significantly reduced tumor burden in all animals compared to the saline control (Fig. 6a). By Day 12, the tumor volume of animals treated with LpCu 3.5 mg/kg and 7.0 mg/kg were reduced by ca. 23% ($p < 0.05$) and 51% ($p < 0.01$) respectively compared to the saline control group. Mice receiving saline liposomes had similar tumor growth rates as the control group, indicating that empty liposomes were not effective and that it is the Cu in LpCu that inhibited tumor growth. The efficacy of $CuCl_2$ was inconclusive because animals either died of copper toxicity or were euthanized at an earlier time point (day 4). No acute signs of toxicity were observed for LpCu at the concentrations administered (Fig. 6b). Sharp decreases in body weight were observed in mice receiving $CuCl_2$ treatment (14% decrease from pre-injection body weight), indicative of acute toxicity for $CuCl_2$ at the 3.5 mg/kg dosing.

Hematology and Blood Biochemistry

Mouse whole blood and serum samples were collected from euthanized mice and analyzed with complete blood counts and several biochemical parameters, including AST, ALT and Cr, were measured (Table 3). The reported serum AST concentration might have been falsely increased due to slight hemolysis during sample collection and preparation; otherwise both AST and ALT concentrations were similar across groups. Cr concentrations were similar among the groups treated with saline, saline liposome, LpCu 3.5 mg/kg and LpCu 7.0 mg/kg, but it was much lower in the $CuCl_2$ group. Although the lack of standard deviation makes it difficult to compare the difference statistically, the results with ELISA assay kits (see supplemental information Table 1s) replicated the same trend. In the hematology parameters, $CuCl_2$ treated mice had less white blood cells, particularly less granulocytes, but increased platelet count and increased platelet hematocrit compared with the control group. These hematologic abnormalities were not observed in LpCu treated mice.

Histology

On Day 12 of animal studies, i.v. treated mice were euthanized and brain, liver, lung, spleen, kidney, eyes and tumor were collected for processing and evaluation by a pathologist at the WVDL (D. Lyman). Liver and spleen were collected because they are the two major organs that preferentially accumulate LUVs (22–24). Eyes, brain and kidney were also collected because they are the organs reported to be most affected by Cu-mediated toxicities other than liver, both in Wilson's disease and other acute Cu intoxication conditions (25–29). Lung was collected because it comprised the largest capillary bed in the animal and is known to be susceptible to ROS damage. Results revealed that there were no pathological

changes in the brain, liver, spleen or lung tissues of Cu treated mice. In the higher dosage group (LpCu 7.0 mg/kg), renal and retinal lesions were observed. Four out of six animals exhibited mild to moderate renal damage, including tubular proteinosis and signs of cellular necrosis (Fig. 7a, 7b). Two of six animals displayed signs of severe apoptotic retinopathy (Fig. 7c), and three out of six animals displayed ocular damage including iridal synechia (Fig. 7d). At the dose of LpCu 3.5 mg/kg, pathological changes were very mild in the eyes and not found in kidney (Fig. 7e, 7f). Mice treated with $CuCl_2$ 3.5 mg/kg displayed similar levels of renal lesions to LpCu 7.0 mg/kg, including renal tubular necrosis, dilation, and the presence of proteinaceous fluid. The histological results are summarized in Table 4. Interestingly, tumors from LpCu treated groups (Fig. 8b) displayed similar levels of mitotic activity and aggressiveness to that of controls (Fig. 8a), and there were no obvious evidences of apoptosis or necrosis in the tumor tissues of all animals.

Tissue Distribution of Cu by Elemental Analysis

Cu concentrations in liver, spleen, kidney, eye and tumor were analyzed by ICP/MS. Only animals receiving three doses of LpCu 3.5 mg/kg and LpCu 7.0 mg/kg were analyzed and compared with controls; animals receiving just one dose of $CuCl_2$ were not analyzed because the deposition of Cu after direct administration has already been reported (25–29). As expected, liver and spleen were the major organs of Cu deposition (Fig. 9) due to preferential accumulation of liposomes into these major organs. There was an 8.4 fold increase of Cu in liver ($p < 0.01$) and 14.6 fold increase of Cu in spleen ($p < 0.01$) in mice treated with LpCu 7.0 mg/kg relative to control. There was a 2.0 fold increase of Cu in liver ($p < 0.01$) and 3.6 fold increase of Cu in spleen ($p < 0.01$) in mice treated with LpCu 3.5 mg/kg relative to control. In tumor tissues, Cu concentration in the LpCu 7.0 mg/kg and LpCu 3.5 mg/kg treatment groups were not statistically different ($p > 0.05$); however with respect to control, there was a 1.3 fold increase of Cu for LpCu 7.0 mg/kg ($p < 0.05$) and 1.4 fold increase of Cu for LpCu 3.5 mg/kg ($p < 0.05$). Kidney and eyes had the most severe Cu-mediated histologically evident damage, but the Cu concentrations in these organs were not elevated by the time the mice were euthanized for tissue collection. Cu concentrations in kidneys of control and all treated groups were not statistically different ($p >0.05$); Cu concentrations in eyes of animals administered LpCu 3.5 mg/kg were not statistically different from controls ($p > 0.05$), but eyes of animals treated with LpCu 7.0 mg/kg had significantly lower Cu concentrations than animals treated with LpCu 3.5 mg/kg or controls ($p < 0.01$).

DISCUSSION

Cu is an essential element found in all living organisms, playing a critical yet complicated role in redox chemistry. Although Cu complexes have been investigated as potential anticancer agents, little attention has been paid to understanding the effect of Cu itself on cell proliferation and tumor inhibition. In this study, we report on the optimized formulation of two Cu salts ($CuCl_2$ and $CuSO_4$) into liposomes and investigated Cu-mediated anticancer properties *in vitro* and *in vivo*, with supporting histology and tissue distribution studies.

Two Cu salts $CuCl_2$ and $CuSO_4$ were investigated for loading into liposomes. Since the aqueous solubility of Cu salts are very high (ca. 620 mg/ml for $CuCl_2$ and 320 mg/ml for $CuSO_4$ at 20°C), there were no solubility issues observed for any of the initial stock Cu concentrations investigated, and these stock solutions were stored at 4°C for several weeks with no evidence of precipitation. Regardless of the initial Cu concentration used for liposomal encapsulation, comparable size, surface charge, PDI, EE and capture volumes of ca. 1.5 μl/μmol total lipids were obtained for all the formulations (Table 1). There were no significant changes in particle size and PDI for all the formulations when liposomes were incubated in FBS at 37 °C for 0, 24, and 48 hours (Table 2), indicative of LpCu formulations' stability in serum. DPPE-PEG_{2000} (5 mole percent with respect to total DPPC) was utilized to formulate stealth liposomes because this percentage was previously reported to cover 100% of the total liposomal surface for optimal colloidal stability and prolonged pharmacokinetics *in vivo* (30). The release profiles were almost identical regardless of the salt form or initial Cu concentration encapsulated in liposomes. For all formulations, there was < 20% Cu released at 25°C after 72 hours and at 37 °C the formulations were characterized by similar half-lives of ca. 30 hours (Fig. 1s). Such consistent release data suggest that all Cu ions were encapsulated within the aqueous core of liposomes and released by diffusion through the lipid bilayer at a constant rate. The release of Cu ions from liposomes was much faster at 37 °C compared to 25 °C (or 4 °C) mainly due to increased lipid fluidity; DPPC has a known phase transition temperature of 41oC although the incorporation of cholesterol into the lipid bilayer is known to increase this transition temperature up to 50 °C (31). The extremely slow release observed at 4 °C made it possible to store LpCu samples for up to two weeks without compromising the formulation properties.

The *in vitro* metabolic cytotoxicity of LpCu formulations was evaluated at 24 and 48 hours on the PC-3 human prostate cancer cell line (Fig. 2). Relatively high concentrations of LpCu and corresponding free copper salts were required before antiproliferative effects were observed (IC_{50} of LpCu and Cu salts ranged from 300–600 μM after 24 hours and ranged from 100–200 μM after 48 hours). When encapsulated in stealth liposomes, cellular uptake of Cu most likely occurred through endocytosis or liposome-cell fusion (32). At identical concentrations, the metabolic toxicities of free Cu salts were very similar to their liposomal-encapsulated formulations. The uptake of free Cu into cells may have been regulated by a set of homeostatic processes involving several Cu-transporter proteins: CTR1 is a high affinity Cu transporter that is responsible for Cu uptake, whereas ATP7A and ATP7B are responsible for Cu export. It has been reported that elevated Cu concentrations can stimulate endocytosis and degradation of CTR1 in A2780, CaCo-2, MDCK, HEK293, HepG2, HeLa cells and primary hepatocytes (33, 34). However, other conflicting reports also reveal no relationship between Cu stimulated endocytosis/degradation of endogenous CTR1 in HEK293 cells (33). Clearly, much is still unknown about Cu homeostasis and its relationship to CTR1 but because expression of the efflux transporter ATP7A has been reported to be endogenously very low in PC-3 cells (35), this may additionally help explain the comparable antiproliferative effects of free Cu and LpCu observed in PC-3 cells.

The intracellular ROS assay demonstrated that when PC-3 cells were incubated with either $CuCl_2$ or LpCu at their IC_{50} concentrations, the intracellular redox homeostasis was

disturbed, resulting in a time-dependent and gradual increase of ROS over 48 hours. The increased production of ROS may have contributed to the decrease in metabolic cell viability observed for LpCu and $CuCl_2$ (Fig. 2) since free radicals can damage DNA, interact with critical proteins and interrupt pathways involved in cellular processes (5). When LpCu and Cu-treated cells were assayed for apoptosis with flow cytometry at 48 and 72 hours (Fig. 4), results confirmed that apoptosis was the primary mechanism of death for LpCu-treated cells after 72 hours, followed closely by cells that also displaying evidence of necrosis; in contrast, free $CuCl_2$ mainly induced apoptosis. This difference may be attributed to the different routes of Cu uptake and trafficking in cells (e.g. liposomal-mediated endocytosis vs. free Cu uptake by copper transporter proteins).

Both i.t. and i.v. administration of LpCu resulted in significant reduced tumor burden in a PC-3 xenograft tumor model compared to saline controls. LpCu treatments successfully localized to the tumor sites since there was a 1.3 fold increase of Cu present in tumor tissues of mice treated with LpCu 7.0 mg/kg and a 1.4 fold increase of Cu in mice treated with LpCu 3.5 mg/kg (Fig. 8). However, the trend of tumor growth rates with respect to time for both i.t. and i.v. experiments indicated that LpCu treatments only decreased overall tumor burden, but had little effect on the tumor growth rate. This may be because the critical intracellular concentration of Cu required to disturb the redox homeostasis of cells could not be achieved in every tumor cell and is a major limiting factor in the anticancer efficacy of Cu-mediated therapy. Histology supports this interpretation since there was no evidence of major tumor tissue damage in the treatment groups (Fig. 8b) compared to control groups (Fig. 8a) in spite of the slightly elevated Cu concentrations.

Evidence of Cu-related toxicity was observed in kidney (Fig. 7a, 7b) and eye (Fig. 7c, 7d). The finding of renal and eye damage agree with several other reports on Cu-mediated toxicities (25–27, 29). Small divalent cations like Cu preferentially undergo renal clearance and it is known that when the amount of Cu exceeds the reserve functional capacity of the kidneys, damage can occur. However, elemental analysis did not detect elevated Cu concentrations in either kidneys or eyes of LpCu-treated animals at 3.5 mg/kg (Fig. 9) at the time of animal euthanasia and organ collection (Day 12). This could be due to a high turnover rate and rapid elimination of severely damaged (and Cu-containing) cells in both kidneys and eyes, but more studies are needed to understand the underlying mechanisms. In contrast, Cu content in eyes of LpCu 7.0 mg/kg dosage group was statistically lower than both control and LpCu 3.5 mg/kg treated groups. This seemingly contradictory result could be due to rapid clearance of damaged cells, and subsequent repair and scarring (leading to the eye lesions observed histologically) at the higher concentration. The glomerular limit of filtration for nanoparticles has been reported to be < 5.5 nm in mice (36). LpCu particles averaging ca. 140 nm could therefore not be renally cleared and the majority of LpCu 3.5 and 7.0 mg/kg doses sequestered in liver and spleen of animals due to preferential uptake by the mononuclear phagocyte system (24). Nevertheless, this increased concentration of Cu did not cause detectable tissue damage in liver and spleen because macrophages have mechanisms for sequestering excess metals (37), in contrast to nearby liver and spleen parenchymal cells. However, it is possible that continued administration of Cu would have eventually led to Cu overloading of macrophages and resulted in detectable signs of tissue damage in liver and spleen over prolonged exposure.

The benefits of liposomal formulation was best demonstrated by the comparison of $CuCl_2$ and LpCu treatment at the same 3.5 mg/kg dose: just one dose of $CuCl_2$ treatment caused 40% of the animals to die shortly after injection, resulted in severe body weight loss in animals that survived, and led to changes in the white blood cell count, total platelet count and decreased blood Cr concentration. In contrast, three repeated doses of LpCu 3.5 mg/kg were well-tolerated. There were only mild pathological changes found in the eyes, and serum creatinine concentrations were within normal limits, indicating that the reserve functional capacity of the kidney had not been exceeded. The serum creatinine concentrations of mice in the LpCu 7.0 mg/kg groups were within normal limits, indicating that they were still functioning well, despite the more severe pathological changes observed histologically. If the mice in the group administered 7.0 mg/kg had been allowed to survive longer, it would be expected that their kidneys would have been able to recover from the toxic effects induced by this dose of LpCu.

CONCLUSION

We have successfully formulated two Cu salts, $CuCl_2$ and $CuSO_4$, into stealth liposomes (LpCu). Both formulations yielded similar loading, and release characteristics, and displayed very little aggregation in serum. Both LpCu and $CuCl_2$ generated *in vitro* metabolic cytotoxicities in PC-3 cells at comparable IC_{50} values. Increasing concentrations of ROS were observed over 48 hours in cells treated with LpCu and $CuCl_2$ at their respective IC_{50} values. A flow cytometry assay revealed that apoptosis was the major mechanism of cell death. Necrosis also contributed to cytotoxicity. LpCu injected as a therapeutic in tumor-bearing mice was effective at reducing overall tumor burden but had little effect on the tumor growth rate. Animals treated at the MTD of LpCu 7.0 mg/kg displayed histologic evidence of toxicity in kidneys and eyes. Tissue distribution of Cu indicated that liver and spleen were the major sites of Cu accumulation.

Supplementary Material

Refer to Web version on PubMed Central for supplementary material.

Acknowledgments

This research was supported by NIH grants R00CA136970 and R01DK099596, and startup funds from the University of Wisconsin-Madison, School of Pharmacy. We are grateful to Professor Manish Patankar and Dr. Arvinder Kapur (Dept. of Ob/Gyn, University of Wisconsin-Madison), and the UWCCC Flow Cytometry Laboratory for invaluable assistance with all the flow cytometry assays. We would also like to thank the WVDL Chemistry Section for performing all the tissue elemental analyses.

Abbreviations

ALT	alanine aminotransferase
AST	aspartate aminotransferase
Cr	creatinine
BCA	bicinchoninic acid

Cu	copper
DDS	drug delivery systems
DF	dilution factor
DLS	dynamic light scattering
DMEM	Dulbecco's Modified Eagle Medium
DPBS	Dulbecco's phosphate buffered saline
EPR	enhanced permeability and retention
FBS	fetal bovine serum
HBSS	Hank's balanced salt solution
HEPES	2-[4-(2-hydroxyethyl)piperazin-1-yl]ethanesulfonic acid buffer
i.t.	intratumoral
i.v.	intravenous
LpCu	stealth formulation of liposomal Cu
LUV	large unilamellar vesicle
MLV	multilamellar vesicle
MTD	maximum tolerated dose
PBS	phosphate buffered saline
PDI	polydispersity index
ROS	reactive oxygen species
TBHP	*tert*-butyl hydroperoxide
WVDL	Wisconsin Veterinary Diagnostic Laboratory

REFERENCES

1. D'Autreaux B, Toledano MB. ROS as signalling molecules: mechanisms that generate specificity in ROS homeostasis. Nat Rev Mol Cell Biol. 2007; 8:813–824. [PubMed: 17848967]
2. Krause KH. Aging: a revisited theory based on free radicals generated by NOX family NADPH oxidases. Exp Gerontol. 2007; 42:256–262. [PubMed: 17126513]
3. Alfadda AA, Sallam RM. Reactive oxygen species in health and disease. J Biomed Biotechnol. 2012; 2012:936486. [PubMed: 22927725]
4. Halliwell B, Gutteridge JM. Role of free radicals and catalytic metal ions in human disease: an overview. Methods Enzymol. 1990; 186:1–85. [PubMed: 2172697]
5. Imlay JA, Chin SM, Linn S. Toxic DNA damage by hydrogen peroxide through the Fenton reaction in vivo and in vitro. Science. 1988; 240:640–642. [PubMed: 2834821]
6. Lu W, Ogasawara MA, Huang P. Models of reactive oxygen species in cancer. Drug Discov Today Dis Models. 2007; 4:67–73. [PubMed: 18591999]
7. Wang Y, Hodgkinson V, Zhu S, Weisman GA, Petris MJ. Advances in the understanding of mammalian copper transporters. Adv Nutr. 2011; 2:129–137. [PubMed: 22332042]

8. Allen PR, Cullis TM. Drug delivery systems: entering the mainstream. Science. 2004; 303:1818–1822. [PubMed: 15031496]
9. Fanciullino R, Ciccolini J. Liposome-encapsulated anticancer drugs: still waiting for the magic bullet? Curr Med Chem. 2009; 16:4361–4371. [PubMed: 19835568]
10. Kawahara K, Sekiguchi A, Kiyoki E, Ueda T, Shimamura K, Kurosaki Y, Miyaoka S, Okabe H, Miyajima M, Kimura J. Effect of TRX-Liposomes Size on Their Prolonged Circulation in Rats. Chemical Pharmaceutical Bulletin. 2003; 51:336–338. [PubMed: 12612425]
11. Wisse E, Jacobs F, Topal B, Frederik P, Geest B. De. The size of endothelial fenestrae in human liver sinusoids: implications for hepatocyte-directed gene transfer. Gene Therapy. 2008; 15:1193–1199. [PubMed: 18401434]
12. Maeda H, Wu J, Sawa T, Matsumura Y, Hori K. Tumor vascular permeability and the EPR effect in macromolecular therapeutics: a review. J Control Release. 2000; 65:271–284. [PubMed: 10699287]
13. Wang Z, Guo T. Copper in medicine: homeostasis, chelation therapy and antitumor drug design. Curr Med Chem. 2006; 13:525–537. [PubMed: 16515519]
14. Marzano C, Pellei M, Tisato F, Santini C. Copper complexes as anticancer agents. Anticancer Agents Med Chem. 2009; 9:185–211. [PubMed: 19199864]
15. Barve V, Ahmed F, Adsule S, Banerjee S, Kulkarni S, Katiyar P, Anson CE, Powell AK, Padhye S, Sarkar FH. Synthesis, molecular characterization, and biological activity of novel synthetic derivatives of chromen-4-one in human cancer cells. J Med Chem. 2006; 49:3800–3808. [PubMed: 16789737]
16. Filomeni G, Cerchiaro G, Da Costa Ferreira AM, De Martino A, Pedersen JZ, Rotilio G, Ciriolo MR. Pro-apoptotic activity of novel Isatin-Schiff base copper(II) complexes depends on oxidative stress induction and organelle-selective damage. J Biol Chem. 2007; 282:12010–12021. [PubMed: 17327230]
17. Awasthi VD, Garcia D, Goins BA, Phillips WT. Circulation and biodistribution profiles of long-circulating PEG-liposomes of various sizes in rabbits. Int J Pharm. 2003; 253:121–132. [PubMed: 12593943]
18. Brenner ED, Harris AJ. A quantitative test for copper using bicinchoninic acid. Anal Biochem. 1995; 226:80–84. [PubMed: 7785783]
19. O'Brien J, Wilson I, Orton T, Pognan F. Investigation of the Alamar Blue (resazurin) fluorescent dye for the assessment of mammalian cell cytotoxicity. Eur J Biochem. 2000; 267:5421–5426. [PubMed: 10951200]
20. Wang JA, Joseph H. Quantifying cellular oxidative stress by dichlorofluorescein assay using microplate reader. Free radical biology & medicine. 1999; 27:612–616. [PubMed: 10490282]
21. Perkins WR, Minchey SR, Ahl PL, Janoff AS. The determination of liposome captured volume. Chem Phys Lipids. 1993; 64:197–217. [PubMed: 8242834]
22. Litzingerand L, Huang DC. Amphipathic poly(ethylene glycol) 5000-stabilized dioleoylphosphatidylethanolamine liposomes accumulate in spleen. Biochimica et Biophysica Acta (BBA) - Lipids and Lipid Metabolism. 1992; 1127:249–254.
23. Gabizon A, Goren D, Horowitz AT, Tzemach D, Lossos A, Siegal T. Long-circulating liposomes for drug delivery in cancer therapy: a review of biodistribution studies in tumor-bearing animals. Advanced Drug Delivery Reviews. 1997; 24:337–344.
24. Allen TM, Hansen C, Rutledge J. Liposomes with prolonged circulation times: factors affecting uptake by reticuloendothelial and other tissues. Biochimica et biophysica acta. 1989; 981:27–35. [PubMed: 2719971]
25. Chugh KS, Sharma BK, Singhal PC, Das KC, Datta BN. Acute renal failure following copper sulphate intoxication. Postgrad Med J. 1977; 53:18–23. [PubMed: 876909]
26. Oldenquist M, Salem G. Parenteral copper sulfate poisoning causing acute renal failure. Nephrol Dial Transpl. 1999; 14:441–443.
27. Dayan MR, Cottrell DG, Mitchell KW. Reversible retinal toxicity associated with retained intravitreal copper foreign body in the absence of intraocular inflammation. Acta Ophthalmologica Scandinavica. 1999; 77:597–598. [PubMed: 10551310]

28. Gaetkeand CK, Chow LM. Copper toxicity, oxidative stress, and antioxidant nutrients. Toxicology. 2003; 189:147–163. [PubMed: 12821289]
29. Galhardi CM, Diniz YS, Faine LA, Rodrigues HG, Burneiko RC, Ribas BO, Novelli EL. Toxicity of copper intake: lipid profile, oxidative stress and susceptibility to renal dysfunction. Food Chem Toxicol. 2004; 42:2053–2060. [PubMed: 15500942]
30. Dos Santos N, Allen C, Doppen AM, Anantha M, Cox KA, Gallagher RC, Karlsson G, Edwards K, Kenner G, Samuels L, Webb MS, Bally MB. Influence of poly(ethylene glycol) grafting density and polymer length on liposomes: relating plasma circulation lifetimes to protein binding. Biochimica et biophysica acta. 2007; 1768:1367–1377. [PubMed: 17400180]
31. Tseng LP, Liang HJ, Chung TW, Huang YY, Liu DZ. Liposomes incorporated with cholesterol for drug release triggered by magnetic field. Journal of Medical and Biological Engineering. 2007; 27:29–34.
32. Düzgüneş S, Nir N. Mechanisms and kinetics of liposome-cell interactions. Advanced Drug Delivery Reviews. 1999; 40:3–18. [PubMed: 10837777]
33. Wang YF, Hodgkinson V, Zhu S, Weisman GA, Petris MJ. Advances in the Understanding of Mammalian Copper Transporters. Adv Nutr. 2011; 2:129–137. [PubMed: 22332042]
34. Petris MJ, Smith K, Lee J, Thiele DJ. Copper-stimulated endocytosis and degradation of the human copper transporter, hCtr1. Journal of Biological Chemistry. 2003; 278:9639–9646. [PubMed: 12501239]
35. White C, Kambe T, Fulcher YG, Sachdev SW, Bush AI, Fritsche K, Lee J, Quinn TP, Petris MJ. Copper transport into the secretory pathway is regulated by oxygen in macrophages. J Cell Sci. 2009; 122:1315–1321. [PubMed: 19351718]
36. Choi HS, Liu W, Misra P, Tanaka E, Zimmer JP, Itty Ipe B, Bawendi MG, Frangioni JV. Renal clearance of quantum dots. Nature biotechnology. 2007; 25:1165–1170.
37. Andrews NC. Disorders of iron metabolism. N Engl J Med. 1999; 341:1986–1995. [PubMed: 10607817]

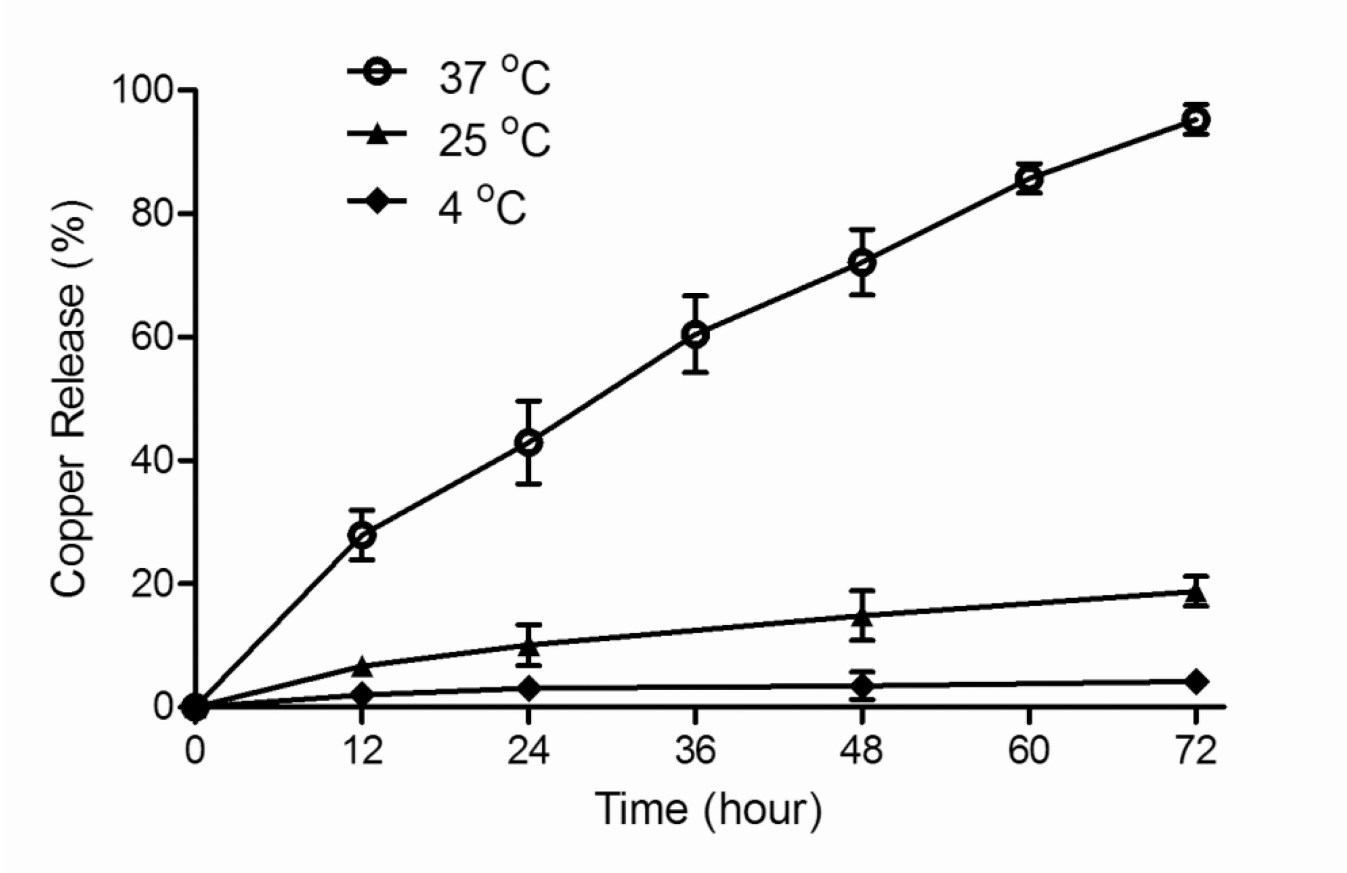

Fig. 1.

In vitro release profiles of Cu from LpCu when dialyzed against 0.9% NaCl at 4oC, 25°C and 37°C. Representative data is shown for LpCu encapsulating ~10 mM Cu prepared from 100 mM $CuCl_2$. Results are nearly identical for all the formulations (see Supplemental Information, Fig. 1s).

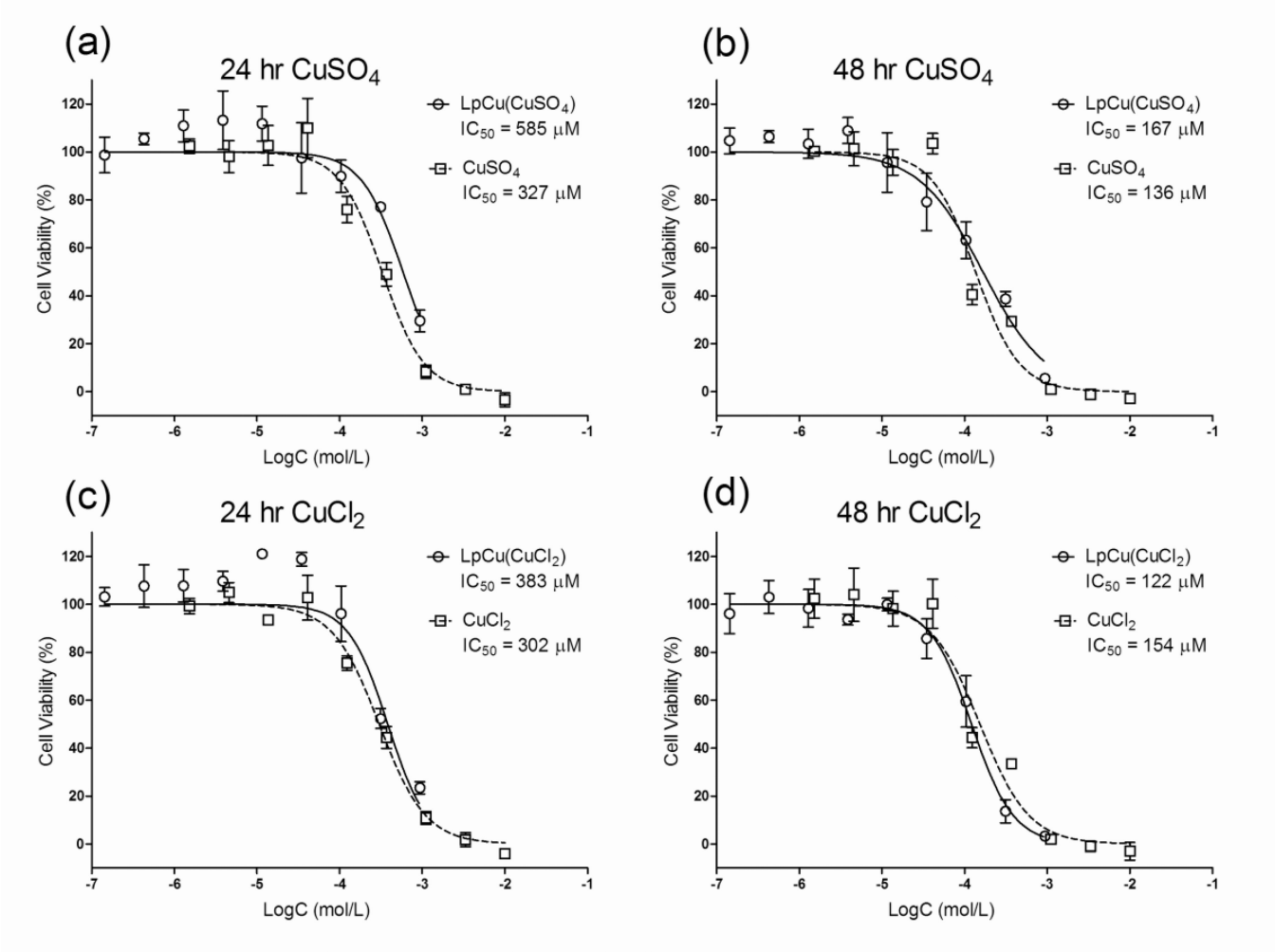

Fig. 2.

Cell metabolic cytotoxicity assay for LpCu and Cu salts ($CuSO_4$ and $CuCl_2$) on PC-3 cells at 24 and 48 hours. One representative result is shown from three independent experiments (N = 3). A logarithmic fit to the raw data was performed to obtain IC_{50} values. At 24 hours, the IC_{50} for LpCu and $CuSO_4$ was 585 uM and 327 μM respectively (**a**). At 48 hours, the IC_{50} for LpCu and $CuSO_4$ was 167 μM and 136 μM respectively (**b**). At 24 hours, the IC_{50} for LpCu and $CuCl_2$ was 383 uM and 302 μM respectively (**c**). At 48 hours, the IC_{50} for LpCu and $CuCl_2$ was 122 μM and 154 μM respectively (**d**). Data points are presented as MEAN ± SEM (n = 4).

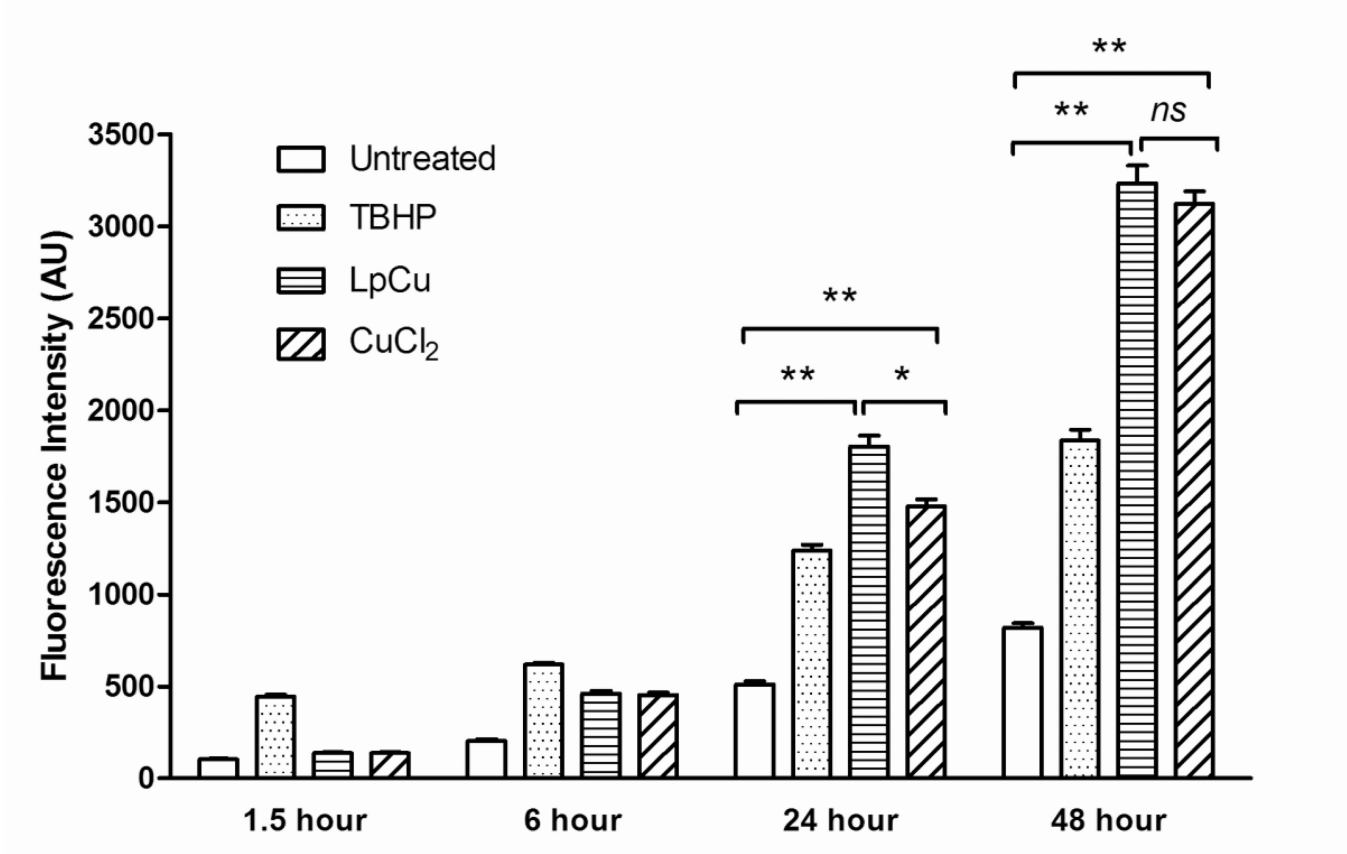

Fig. 3.

Intracellular ROS concentrations at 1.5, 6, 24 and 48 hours in untreated PC-3 cells and PC-3 cells treated with TBHP at 100 μM, $CuCl_2$ at 154 μM, or LpCu at 122 μM. Fluorescence intensity results are normalized with respect to total protein concentration. One representative result is shown from three independent experiments (N = 3). At 24 and 48 hours, there were statistical differences in ROS levels between untreated cells and LpCu, and untreated cells and $CuCl_2$. There was also a significant difference in ROS levels between LpCu and $CuCl_2$ at 24 hours, but at 48 hours the difference became insignificant. Results presented are MEAN ± SEM of arbitrary units (n = 8). * $p < 0.05$, ** $p < 0.01$, *ns* means not significant.

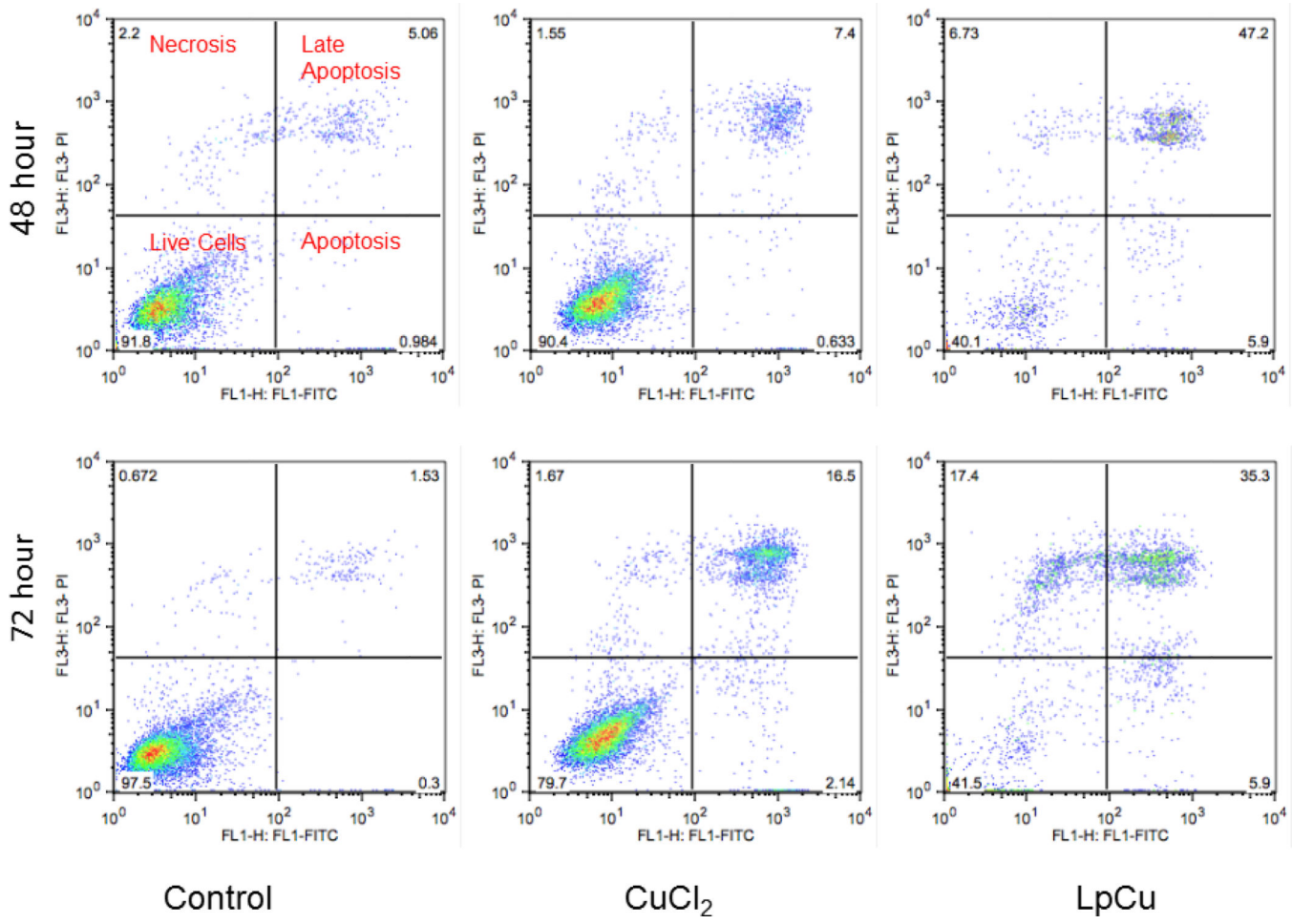

Fig. 4.

After 48 and 72 hours incubation with either 122 μM LpCu or 154 μM $CuCl_2$, cells were stained with Annexin V-FITC and propidium iodide, probed for both apoptosis and necrosis by flow cytometry (n = 20,000 cells gated for each group). One representative result is shown from three independent experiments (N = 3).

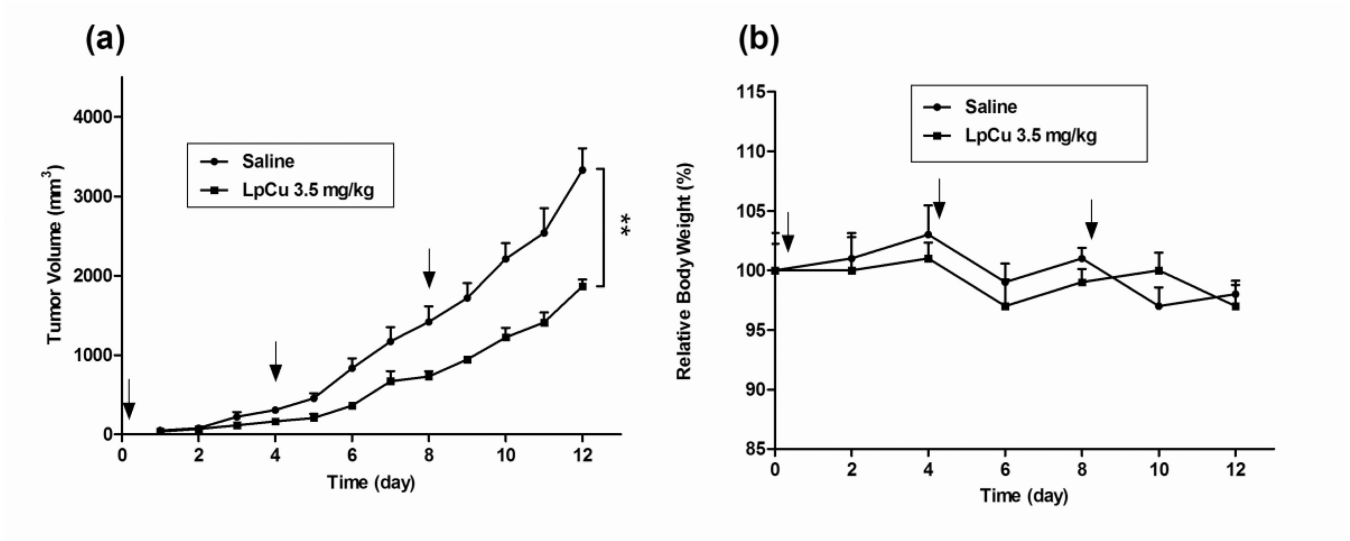

Fig. 5.

PC-3 tumor-bearing mice were injected i.t. with either saline or LpCu at a dose of 3.5 mg/kg on Days 0, 4, and 8. Tumors (**a**) and body weights (**b**) of animals were measured daily. By Day 12, the tumor volume of LpCu 3.5 mg/kg group was 44% smaller than control group. Results presented are MEAN ± SEM (n=4); ** $p<0.01$.

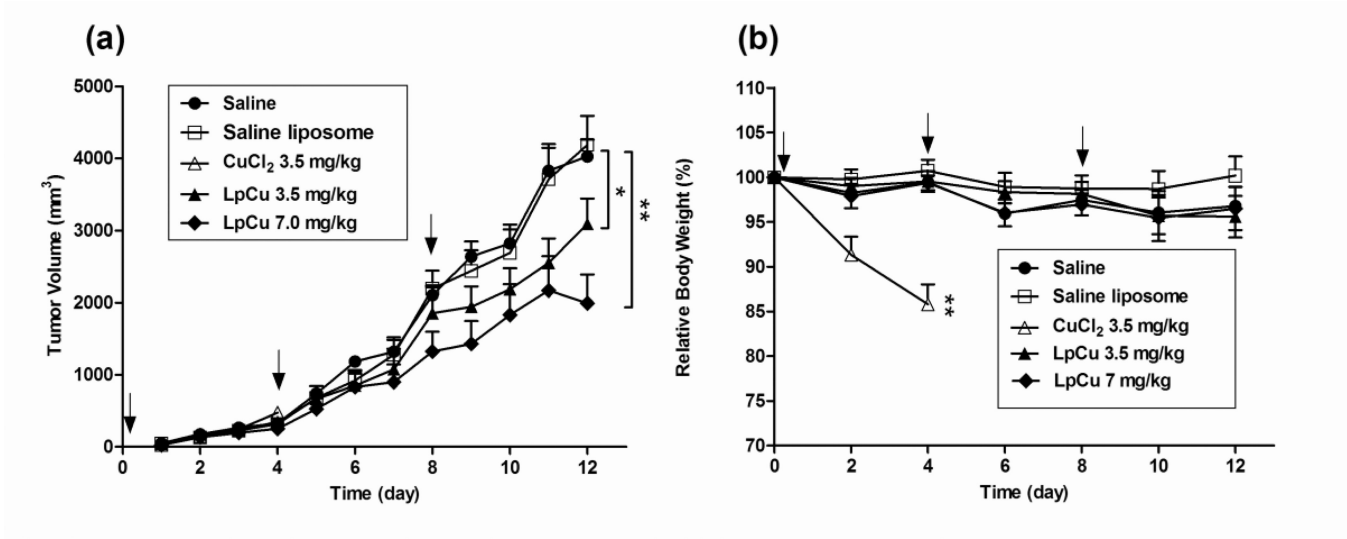

Fig. 6.

PC-3 tumor-bearing mice were injected i.v. with saline, saline liposome, $CuCl_2$ at 3.5 mg/kg or LpCu at a dose of 3.5 or 7.0 mg/kg (n = 5 or 6) on Days 0, 4, and 8. Two independent experiments were conducted (N = 2), of which one representative result is shown. Tumors (**a**) and body weights (**b**) of animals were measured daily. By Day 12, the tumor volumes of LpCu 3.5 mg/kg and LpCu 7.0 mg/kg were 23% and 51% smaller respectively than control animals injected with saline; 2 out of 5 mice in the $CuCl_2$ 3.5 mg/kg group died by Day 3, and the remaining 3 mice in the group were euthanized on Day 4 due to severe signs of acute toxicities. Results presented are MEAN ± SEM (n = 3 for $CuCl_2$ 3.5 mg/kg group, n = 6 for all other groups); * $p<0.05$, ** $p<0.01$.

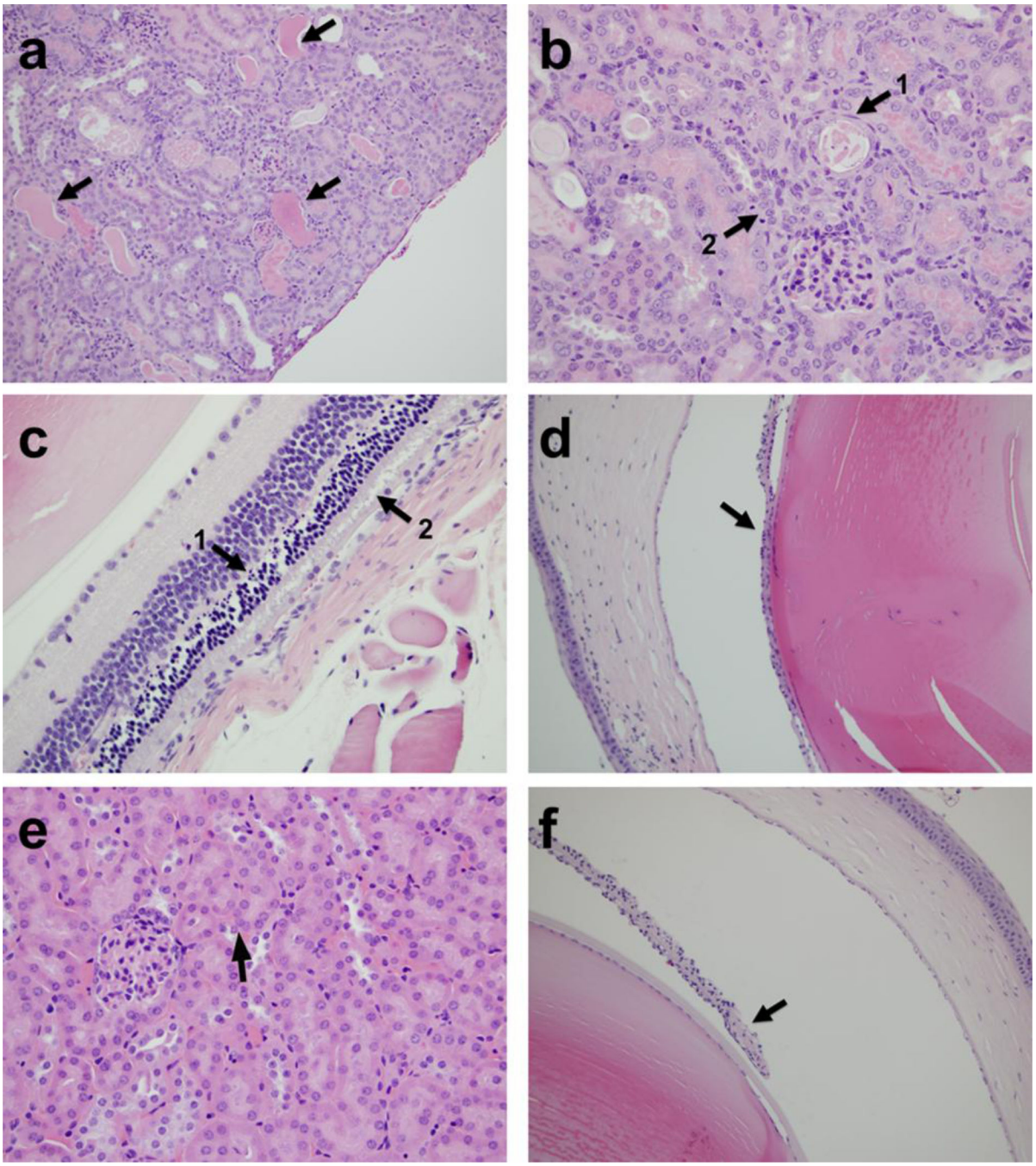

Fig. 7.

Histological findings in kidneys and eyes of LpCu-treated mice. Arrows point to dilated tubules filled with protein and necrotic materials in kidney of LpCu 7.0 mg/kg treated group (**a**); arrow 1 points to a necrotic tubule containing a flattened epithelial cell nucleus and arrow 2 points to a mitotic figure indicative of post-damage tubular regeneration in kidney of LpCu 7.0 mg/kg treated group (**b**); arrow 1 points to apoptotic debris within the outer nuclear cell layer and arrow 2 points to evidence of photoreceptor disruption in eye of LpCu 7.0 mg/kg treated group (**c**); arrow points to the iris adhering to the lens capsule, i.e.

posterior synechia, in eye of LpCu 7.0 mg/kg treated group (**d**); arrow points to normal kidney tubules and cell morphology in kidney of LpCu 3.5 mg/kg treated group (**e**); arrow points to the iris not attached to the lens capsule, i.e. indicative of eye morphology within normal limits, in eye of LpCu 3.5 mg/kg treated group (**f**).

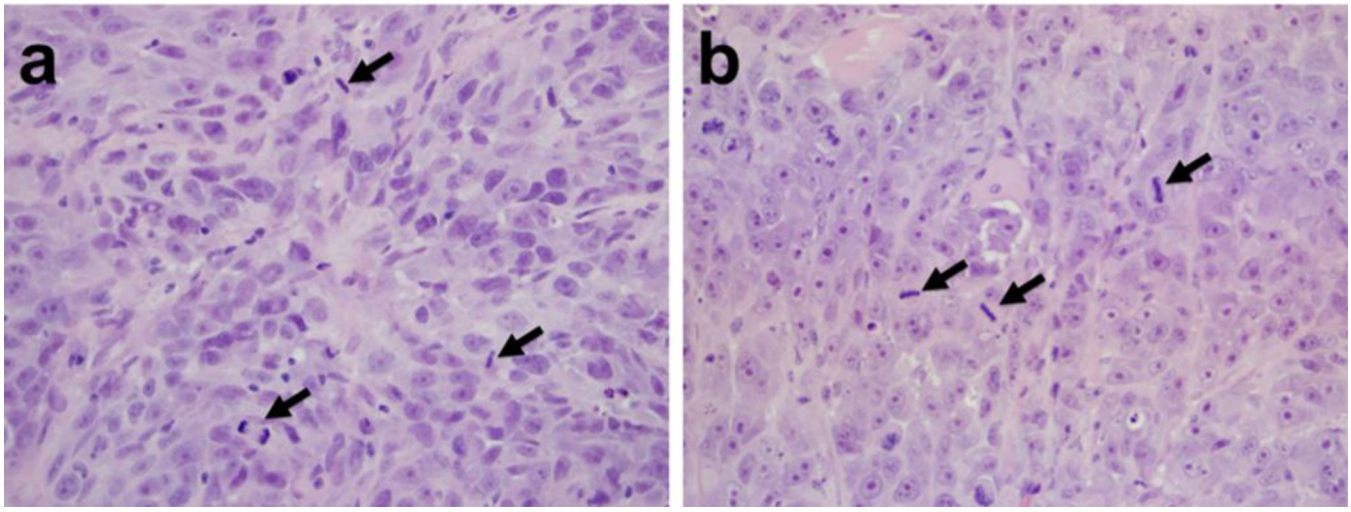

Fig. 8.

Tumor histology of saline (**a**) and LpCu 7.0 mg/kg (**b**) treated animals. Several arrows point to evidence of mitotic cells in the tumors, indicative of similar levels of tumor aggressiveness irrespective of treatment modalities.

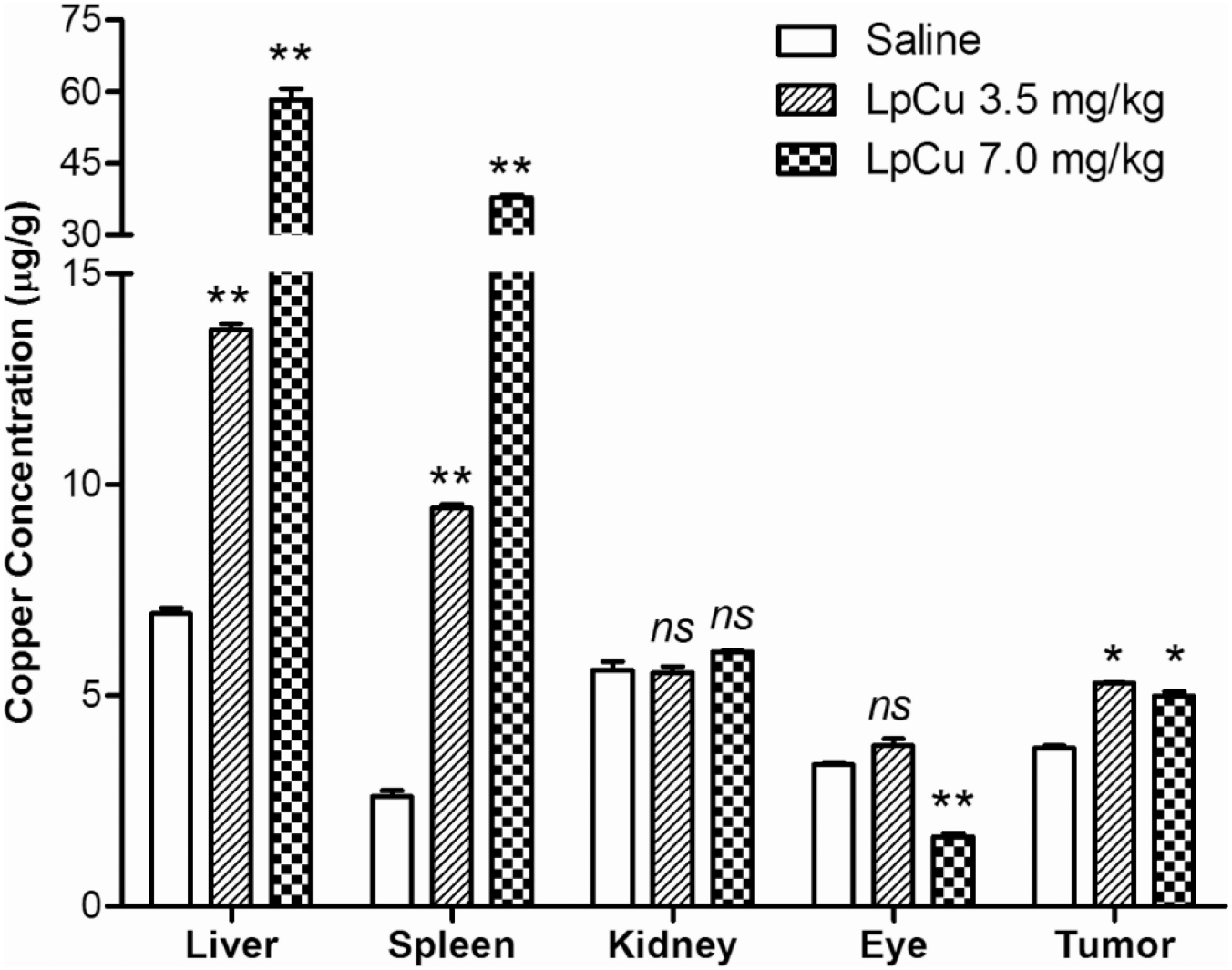

Fig. 9.

Tissues of animals treated i.v. with either saline, LpCu 3.5, or LpCu 7.0 mg/kg were collected and pooled at the end of the study. Pooled liver, spleen, kidney, eye and tumor tissues were analyzed for Cu content by ICP/MS. Results presented are MEAN ± SEM (n = 3 replicate analysis); * $p<0.05$, ** $p<0.01$, *ns* means not significant.

Table 1

Characterization of LpCu Prepared from Different Concentrations of $CuCl_2$ and $CuSO_4$

Salt Form	Conc. (mM)	Size (nm)	PDI	Zeta-Potential (mV)	EE (%)
$CuCl_2$	100	141.8±1.5	0.071±0.007	−8.50±0.44	19.3±0.7
	200	145.3±1.3	0.071±0.014	−8.78±0.08	18.7±0.5
	300	147.2±1.6	0.069±0.018	−10.11±0.60	21.6±1.1
	400	151.5±1.2	0.075±0.007	−6.36±0.06	20.9±0.7
	500	153.8±2.8	0.091±0.032	−7.29±0.30	19.2±1.0
$CuSO_4$	100	142.5±0.6	0.053±0.023	−9.86±0.29	20.9±1.1
	200	144.4±1.4	0.062±0.020	−10.29±0.88	21.5±0.5
	300	145.9±0.9	0.057±0.001	−7.33±0.66	19.9±1.8
	400	145.0±1.2	0.091±0.028	−6.45±0.58	21.3±1.1
	500	150.5±1.8	0.080±0.010	−6.56±0.36	21.0±0.3

Table 2

Colloidal Stability of LpCu Incubated with Pure FBS at 37°C

Salt Form	Conc. (mM)	0 hour		24 hour		48 hour	
		Size (nm)	PDI	Size (nm)	PDI	Size (nm)	PDI
$CuCl_2$	100	159.2±1.0	0.187±0.011	157.4±0.5	0.166±0.007	163.8±3.0	0.175±0.005
	200	161.2±0.7	0.182±0.003	157.4±0.4	0.177±0.005	161.7±1.8	0.182±0.004
	300	166.9±0.8	0.167±0.014	157.3±1.4	0.180±0.018	159.0±2.3	0.195±0.010
	400	164.2±1.0	0.160±0.003	161.7±0.4	0.170±0.007	162.2±1.4	0.166±0.021
	500	164.4±0.4	0.157±0.006	164.4±2.0	0.182±0.004	163.5±2.5	0.184±0.005
$CuSO_4$	100	160.9±1.4	0.148±0.013	160.9±1.4	0.140±0.008	162.2±1.6	0.158±0.007
	200	154.5±1.3	0.194±0.015	153.8±2.3	0.201±0.025	155.0±1.4	0.217±0.013
	300	168.6±0.8	0.158±0.018	167.8±1.6	0.167±0.019	168.7±2.8	0.166±0.009
	400	170.8±2.2	0.143±0.013	171.3±1.5	0.154±0.031	169.7±0.4	0.168±0.007
	500	178.9±1.8	0.151±0.012	178.4±1.0	0.152±0.007	177.7±2.1	0.137±0.011

Table 3

Complete Blood Biochemistry and Hematology

	Saline	**Saline liposome**	**LpCu 3.5 mg/kg**	**LpCu 7.0 mg/kg**	**$CuCl_2$ 3.5 mg/kg**
Biochemistry					
AST (U/L)	568	386	873	573	176
ALT (U/L)	110	252	140	87	86
Cr (mg/dL)	0.4	0.4	0.5	0.4	0.2
Hematology					
WBC (K/μL)	23.2 ± 8.3	27.6 ± 6.0	20.0 ± 6.6	15.2 ± 4.9	10.6 ± 1.0 *
LYM (K/μL)	6.2 ± 1.9	7.9 ± 2.4	8.9 ± 3.0	7.1 ± 2.8	4.4 ± 1.6
MON (K/ML)	1.3 ± 0.6	1.9 ± 0.4	1.1 ± 0.6	1.1 ± 0.3	0.5 ± 0.2
GRA (K/μL)	15.7 ± 7.3	17.7 ± 4.0	10.2 ± 3.3	7.1 ± 1.3	5.7 ± 0.3 *
RBC (M/μL)	8.7 ± 1.5	9.0 ± 0.3	8.8 ± 0.4	9.2 ± 0.6	9.8 ± 1.3
HGB (g/dL)	14.0 ± 2.4	14.9 ± 0.7	14.1 ± 0.8	14.9 ± 0.7	15.7 ± 1.8
HCT (%)	43.2 ± 7.3	43.8 ± 1.8	45.9 ± 0.6	44.0 ± 2.5	46.7 ± 4.3
MCV (fL)	49.6 ± 4.2	48.6 ± 2.9	52.2 ± 2.7	48.2 ± 1.5	47.3 ± 2.1
MCH (pg)	16.0 ± 0.9	16.5 ± 0.9	16.0 ± 0.9	16.2 ± 0.5	15.8 ± 0.4
MCHC (g/dL)	32.4 ± 1.4	33.9 ± 1.4	30.7 ± 1.0	33.8 ± 0.8	33.4 ± 0.8
PLT (K/ML)	429 ± 99	464 ± 69	440 ± 133	546 ± 44	989 ± 148 *
MPV (fL)	10.2 ± 2.1	7.0 ± 0.2	7.2 ± 0.3	9.1 ± 2.2	7.8 ± 0.6
PCT (%)	0.37 ± 0.04	0.32 ± 0.04	0.32 ± 0.09	0.38 ± 0.03	0.76 ± 0.17 *

Abbreviations: AST, aspartate aminotransferase; ALT, alanine aminotransferase; Cr, creatinine; WBC, white blood cell (leukocyte); LYM, lymphocyte; MON, monocyte; GRA, granulocyte; RBC, red blood cell; HGB, hemoglobin; HCT, hematocrit; MCV, mean corpuscular volume; MCH, mean corpuscular hemoglobin; MCHC, mean corpuscular hemoglobin concentration; PLT, total platelet count; MPV, mean platelet volume; PCT, platelet hematocrit. Biochemistry was measured from pooled serum samples within the same group, hence no standard deviation is shown (for ELISA analysis of the same parameters with standard deviations, see supplemental information Table 1s); Hematology results are MEAN ± SD (n=3 for $CuCl_2$ group and n=5 for other groups).

* $P < 0.05$.

Table 4

Pathological Changes and Severeness in Experimental Animals

	Saline	Saline liposome	LpCu 3.5 mg/kg	LpCu 7.0 mg/kg	$CuCl_2$ 3.5 mg/kg *
Posterior synechia (eye)	−	−	+	+++	−
Photoreceptor degeneration (eye)	−	−	+	++	−
Outer nuclear layer apoptosis (eye)	−	−	+	++	−
Renal tubular necrosis and dilation	−	−	−	++++	++++
Renal tubular proteinaceous fluid	−	−	−	+++	++++
Renal hemorrhage	−	−	−	+	−

* Two out of five mice died spontaneously after one dose of $CuCl_2$ 3.5 mg/kg, and the rest three were euthanized immediately.

+ and −, degree / frequency of pathological changes; −, no pathological changes; +, mild; ++, moderate; +++, severe; ++++, extremely severe.